Water-Soluble β-Sheet Models Which Self-Assemble into Fibrillar Structures[†]

Katharina Janek,*[,‡] Joachim Behlke,[§] Josef Zipper,[‡] Heinz Fabian,[§] Yannis Georgalis,[||] Michael Beyermann,[‡] Michael Bienert,[‡] and Eberhard Krause[‡]

Institute of Molecular Pharmacology, Max Delbrück Center of Molecular Medicine, and Institute of Crystallography, Free University, Berlin, Germany

Received March 3, 1999; Revised Manuscript Received April 19, 1999

ABSTRACT: Self-assembly of β-sheet domains resulting in the formation of pathogenic, fibrillar protein aggregates (amyloids) is a characteristic feature of various medical disorders. These include neurodegenerative diseases, such as Alzheimer's, Huntington's, and Creutzfeldt−Jacob's. A significant problem in studying such aggregation processes is the poor solubility of these β-sheet complexes. The present work describes water-soluble de novo β-sheet peptides which self-assemble into fibrillar structures. The model peptides enable studies of the relationship between β-sheet stability and association behavior. The peptides [DPKGDPKG-$(VT)_n$-GKGDPKPD-NH_2, $n = 3-8$] are composed of a central β-sheet-forming domain (VT-sequence), and N- and C-terminal nonstructured octapeptide sequences which promote water solubility. Conformational analyses by circular dichroism and Fourier transform infrared spectroscopy indicate the influence of peptide length, D-amino acid substitution, and concentration on the ability of the peptides to form stable β-sheet structures. The association behavior investigated by analytical ultracentrifugation and dynamic light scattering was found to correlate strongly with the stability of a β-sheet conformation. Model peptides with $n \geq 6$ form stable, water-soluble β-sheet complexes with molecular masses of more than 2000 kDa, which are organized in fibrillar structures. The fibrils examined by Congo Red staining and electron microscopy show some similarities with naturally occurring amyloid fibrils.

Self-assembly of β-sheet domains resulting in the formation of ordered fibrillar structures is a common feature of various medical disorders. These include infectious prion diseases, e.g., bovine spongiform encephalopathy or Creuzfeldt−Jacob disease (*1*), amyloidoses, such as Alzheimer's disease or type II diabetes (*2*), and Huntington's disease (*3*). Characteristic for these diseases is that amyloidogenic precursor proteins are converted into insoluble pathogenic protein fibrils (amyloids). Although the proteins involved have no sequential or structural similarities, the aggregates formed are remarkably similar with regard to their morphological and tinctorial properties and consist predominantly of β-sheet structures (*2*, *4*). Although the pathogenic mechanisms of fibril formation are not yet fully understood, a common theme for all amyloids has been suggested (*5*). Sequences of the normally folded proteins undergo conformational changes, resulting in β-sheet structured intermediates, which are capable of self-assembling into highly aggregated fibrils (*5*, *6*). Several studies have shown that the extent of β-sheet formation is directly correlated with the ability to form amyloid fibrils (*7*). Sequence modifications of βA4 peptide fragments characteristic of Alzheimer's disease, which show a decrease of β-sheet conformation, are less fibrilliogenic in character (*8*−*14*). Point mutation, as found in the Dutch type of βA4 (^{22}Glu → Gln), resulted in a higher β-sheet content and accelerated fibril formation (*15*, *16*). Self-assembly into fibrillar β-sheet complexes has also been reported for other peptides/proteins, which are not associated with medical disorders. Such systems are derived either from naturally occurring proteins or from designed sequences (*17*−*26*). On the other hand, unlike α-helices, β-sheet domains are a much less intensively studied type of secondary structure. A significant problem in studying these structures and their self-organization into fibrillar structures is the poor solubility of the intermolecularly associated β-strands. To broaden our understanding of β-sheet formation, stabilization, and association/aggregation, well-defined soluble peptide models were designed as useful tools in simplifing the studies of these complex processes. Such systems might also allow the development of strategies for the inhibition of either β-sheet formation or the association into fibrillar β-sheet complexes. On the basis of previous work (*27*), the designed peptides [DPKGDPKG-$(VT)_n$-GKGDPKPD-NH_2, $n = 3-8$] are composed of a central β-sheet-forming domain (VT-sequence) of various lengths, located between N- and C-terminal unstructured octapeptide sequences which promote water solubility. To destabilize the β-structure in a site-specific manner without changing other properties of the peptides, such as hydrophobicity, side chain functionality, or charge distribution, we included double D-amino acid-substituted analogues (for sequences see Table 1). Both the length of the secondary structure domain and

[†] This work was supported by the Deutsche Forschungsgemeinschaft Kr 1451/2-2.

* Address correspondence to this author at Forschungsinstitut für Molekulare Pharmakologie, AlfredKowalke-Strasse 4, 10315 Berlin, Germany. E-mail: janek@fmp-berlin.de. Tel: +49-30-51551344. Fax: +49-30-51551206.

[‡] Institute of Molecular Pharmacology.

[§] Max Delbrück Center.

[||] Institute of Crystallography, Free University.

10.1021/bi990510+ CCC: $18.00
Published on Web 06/06/1999

Table 1: Synthetic $(VT)_n$-Peptides Used in This Study

$(VT)_n$-Peptide		Sequence[a]	Residues in the β-Sheet Forming Domain	D-Amino Acid Substitution
VT3	n = 3	DPKGDPKG**VTVTVT**.....GKGDPKPD-NH_2	6	none
VT4	n = 4	DPKGDPKG**VTVTVTVT**.....GKGDPKPD-NH_2	8	none
VT5	n = 5	DPKGDPKG**VTVTVTVTVT**.....GKGDPKPD-NH_2	10	none
VT5-DD		DPKGDPKG**VTVTvtVTVT**.....GKGDPKPD-NH_2	10	v13 t14
VT6	n = 6	DPKGDPKG**VTVTVTVTVTVT**....GKGDPKPD-NH_2	12	none
VT6-DD		DPKGDPKG**VTVTVTvtVTVT**....GKGDPKPD-NH_2	12	v15 t16
VT7	n = 7	DPKGDPKG**VTVTVTVTVTVTVT**..GKGDPKPD-NH_2	14	none
VT7-DD		DPKGDPKG**VTVTVTvtVTVTVT**..GKGDPKPD-NH_2	14	v15 t16
VT8	n = 8	DPKGDPKG**VTVTVTVTVTVTVTVT**GKGDPKPD-NH_2	16	none
VT8-DD		DPKGDPKG**VTVTVTVTvtVTVTVT**GKGDPKPD-NH_2	16	v17 t18

[a] D-Amino acids are printed in lowercase letters.

the influence of D-amino acid substitution were correlated with the β-sheet stability and the association behavior. It was shown that strong association of β-strands results in fibrillar structures which are able to bind Congo Red (CR)[1] and exhibit birefringence.

MATERIALS AND METHODS

Peptide Synthesis and Purification. DPKGDPKG-$(VT)_n$-GKGDPKPD-NH_2 ($n = 3-8$) and the corresponding D-amino acid analogues (see Table 1) were synthesized by solid-phase methods on an automated MilliGen 9050 peptide synthesizer (Milligen/Biosearch, Burlington, MA) using Fmoc (N^{α}-9-fluorenylmethoxycarbonyl) chemistry in the continuous flow mode: TentaGel S RAM resin, 0.22 mmol/g (Rapp Polymere, Tübingen, Germany), HBTU (*N*-[(1*H*-benzotriazol-1-yl)(dimethylamino)methylene]-*N*-methylmethaminium hexafluorophosphate *N*-oxide), 2 equiv of DIEA (diisopropylethylamine), coupling time 20 min, and deblocking time with 20% piperidine in DMF (dimethylformamide) 10 min. Amino acids in the VT-region were double coupled. The peptides were cleaved from the resin support by 95% trifluoroacetic acid/5% water for 3 h. The crude peptides were purified by preparative reversed-phase chromatography on PolyEncap A300 (10 μm, 250 × 20 mm i.d., Bischoff Analysentechnik GmbH, Leonberg, Germany), using an acetonitrile/water−0.1% trifluoroacetic acid solvent system. The purified peptides (>95% according to HPLC analysis) were characterized by MALDI mass spectroscopy (Voyager-DE STR, Perseptive Biosystems, Framingham, MA) using a sinapinic acid matrix, which gave the expected $[M + H]^+$ mass peaks for each peptide. The peptide content of lyophilized samples was determined by quantitative amino acid analyses (LC 3000 analyzer, Biotronik-Eppendorf, Maintal, Germany). Because the trifluoroacetate counterion gives rise to a strong band at ~1673 cm^{-1} in the infrared spectrum which overlaps the conformation-sensitive amide I band of the peptide backbone, all such counterions were replaced by chloride ion by lyophilization twice from 10 mM hydrochloric acid.

[1] Abbreviations: CR, Congo Red; CD, circular dichroism; FTIR, Fourier transform infrared.

Circular Dichroism Measurements. Circular dichroism (CD) spectra were measured at 25 °C on a J-720 spectropolarimeter (Jasco, Tokyo, Japan), in a quartz cell of 0.1 cm path length, over the range 190−260 nm. The instrument was calibrated with an aqueous solution of (+)-10-camphorsulfonic acid. CD spectra were the average of a series of five to eight scans made at 0.1 nm intervals. Peptide concentrations were 5×10^{-5} and 1×10^{-4} M in aqueous solution. The CD results are reported as mean residue molar ellipticity [Θ] in deg cm^2/dmol.

Guanidine hydrochloride titration was performed by mixing stock solutions of the peptide and 8 M guanidine hydrochloride, both in buffer (75 mM sodium phosphate, pH 4.4). The resulting peptide concentration of 5×10^{-5} M was titrated against increasing guanidine hydrochloride concentrations up to 7.8 M. Temperature denaturation experiments were carried out at a peptide concentration of 5×10^{-5} M in aqueous solution in the range 25−85 °C.

Fourier Transform Infrared Spectroscopy. Infrared spectra were collected on a IFS-66 FTIR (Bruker, Karlsruhe, Germany) spectrometer equipped with a DT65 detector and continuously purged with dry air. Measurements were performed in 30 mM sodium phosphate buffer with D_2O (pH 2.2). All data were obtained from freshly prepared solutions at peptide concentrations of 0.5 and 5×10^{-3} M. The samples were placed between a pair of CaF_2 windows separated by a path length of 50 μm. The solvent spectrum was recorded under identical conditions and subtracted from the peptide spectra. For each sample, 128 or 256 interferrograms were coadded, and Fourier transformed, to generate a spectrum with a nominal resolution of 4 cm^{-1}. Residual water vapor was interactively subtracted, as described earlier (*28*). The final unsmoothed peptide spectra were used for further analysis. Band narrowing of the spectra by Fourier self-deconvolution, which leads to a better visualization of overlapping bands, was carried out using a half-bandwidth of 16 cm^{-1} and a band narrowing factor $k = 1.6$.

Analytical Ultracentrifugation. Peptides (1 mg/mL) were dissolved in 30 mM sodium phosphate, pH 4.4, containing 0.9% sodium chloride, and the solutions were centrifuged at 20 °C in standard double sector cells using an analytical ultracentrifuge XL-A (Beckman, Palo Alto, CA). The time-

dependent moving boundaries recorded at 225 nm were fit simultaneously, using the program LAMM (*29*), to obtain the sedimentation (s) and diffusion coefficients (D). From these parameters, and the partial specific volume ($\bar{\nu}$) derived from the amino acid composition and the corresponding density increments (*30*), the molecular mass of the various peptides was calculated using the Svedberg equation. In addition, from the data mentioned the frictional ratio (f/f_0) of the samples was derived as an indicator of the gross conformation of the peptides examined.

Dynamic Light Scattering. Dynamic light scattering measurements were performed in an experimental setup equipped with a 2W Spectra Physics 2017 Ar^+ laser (488 nm), an ALV/SP-86 spectrogoniometer (ALV, Langen, Germany), and the ALV-FAST/5000/E digital autocorrelation boards. The scattering angle was 30°, the temperature being 20.0 ± 0.1 °C. Peptide and buffer (30 mM sodium phosphate, pH 4.4) were mixed rapidly (peptide concentration 2×10^{-4} M) and filtered through Ministart sterile filters (200 nm pore size) into a standard cylindrical light scattering cell. The data collection began within less than 1 min after mixing.

Light Microscopy. Ten microliters of an aqueous peptide solution (1 mg/mL) was placed on a microscope slide, air-dried at 50 °C, and stained with a saturated solution of CR in 80% ethanol (20 min). After being washed with water, 80% ethanol, absolute ethanol, and water, the stained sample was examined under a microscope with bright and polarized light (magnification 400×).

Electron Microscopy. Peptides were dissolved in water at a concentration of 2×10^{-4} M, stored at room temperature for 24 h, and absorbed onto 200-mesh carbon-coated copper grids. A 5-μL aliquot was absorbed for 60 s. Excess liquid was then removed with filter paper. The wet sample on the grid was negatively stained with 5 μL of a freshly prepared solution of 2% (w/v) uranyl acetate in water. After 60 s the excess liquid was removed, and the sample was allowed to air-dry. Specimens were examined with a 902 A electron microscope (Zeiss, Oberkochen, Germany) at 80 kV.

RESULTS

Peptide Conformation. CD studies of $(VT)_n$-peptides in aqueous solution suggest differing potentials of the peptides to form β-sheet structures. Short peptides with six and eight residues in the central domain (VT3 and VT4) are unstructured, as indicated by CD spectra showing a minimum of the molar ellipticity at 198 nm and no positive feature (traces a and b in Figure 1 A). The addition of two further residues (VT5) results in a slightly red-shifted CD spectrum (Figure 1A, trace c), which indicates the beginning of a transition from a random coil to an ordered structure. With elongation of the VT-domain to 12−16 residues (VT6−VT8), the conversion is complete. The CD spectra of these peptides are characterized by a negative band at 214 nm and a positive band at 192 nm, which is typical of a β-sheet conformation. The increasing intensities of the CD spectra of VT6 and VT7/VT8 (Figure 1A, traces d−f) indicate stabilization of the β-structure by elongation of the VT-domain. Monomeric or low molecular weight β-sheets exhibit a mean residue ellipticity of approximately $(-10 \pm 2) \times 10^3$ at 215 ± 5 nm. Considerably higher values than this appear to result from large intermolecularly associated β-sheet structures (*31*).

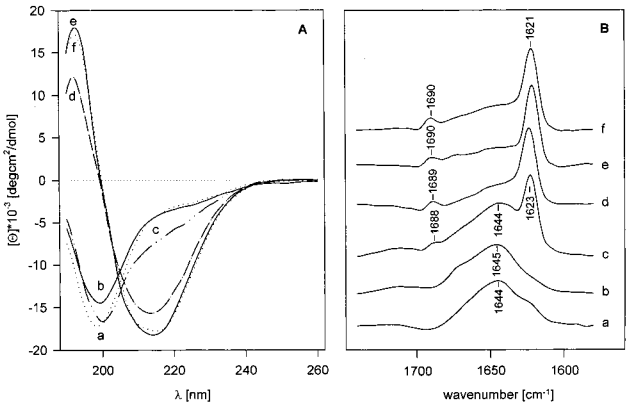

FIGURE 1: Conformation of $(VT)_n$-peptides [VT3 (a), VT4 (b), VT5 (c), VT6 (d), VT7 (e), VT8 (f)] investigated by CD (A) in water at a peptide concentration of 5×10^{-5} M and FTIR (B) in D_2O buffer (30 mM sodium phosphate, pH 2.2) at a peptide concentration of 5×10^{-4} M. The FTIR spectra in the amide I region are shown after Fourier self-deconvolution.

Consequently, the high mean residue ellipticities between -16×10^3 and -18×10^3, measured for VT6 and VT7/VT8, respectively, suggest that these peptides are highly associated.

The conversion from random coil to β-sheet conformation caused by the addition of only one VT-repeat from VT5 to VT6 was confirmed by Fourier transform infrared (FTIR) spectroscopy. The spectra recorded at 5×10^{-4} M are depicted in Figure 1B. The spectra of VT3 and VT4 (Figure 1B, traces a and b) are characterized by a broad, structureless amide I band centered at 1644−1645 cm^{-1}, which is typical for peptides having no regular secondary structure. The spectrum of the VT5 peptide (Figure 1B, trace c) reveals two additional features: a strong band at 1623 cm^{-1} and a weak band at 1688 cm^{-1}. These two bands are highly characteristic of antiparallel β-sheet structures, which grow upon increasing the peptide concentration to 6×10^{-3} M (*27*). The β-structure bands are the dominant features in the spectra of the VT6, VT7, and VT8 peptides (Figure 1B, traces d−f). In addition, there is an increase in band splitting (65 cm^{-1} for VT5 versus 69 cm^{-1} for VT8) between the low- and high-frequency β-sheet amide I band components, suggesting that the β-sheet structure of the VT8 peptide is experiencing stronger hydrogen bonding. A change in peptide concentration from 5×10^{-4} to 5×10^{-3} M has no impact on the spectra of these peptides.

The high stability of the intermolecular β-sheet structures of VT6, VT7, and VT8 was proved by guanidine hydrochloride and temperature denaturation. Increasing the guanidine hydrochloride concentration to 7.2 M in 75 mM sodium phosphate buffer, pH 4.4, or increasing the temperature to 85 °C caused no significant effect on the CD spectra of these peptides (data not shown).

Influence of D*-Amino Acid Substitution on the β-Sheet Conformation.* Double D-amino acid substitution was previously found to destabilize α-helices (*32*, *33*) and weak β-sheet structures (*27*). To evaluate D-amino acid substitution on more stable β-sheet structures, VT-peptide analogues having two such adjacent substitutions in the center of the molecule were studied (for sequences see Table 1). The CD spectra of the peptides VT6-DD, VT7-DD, and VT8-DD are shown in Figure 2A. The CD spectrum of the VT6-DD

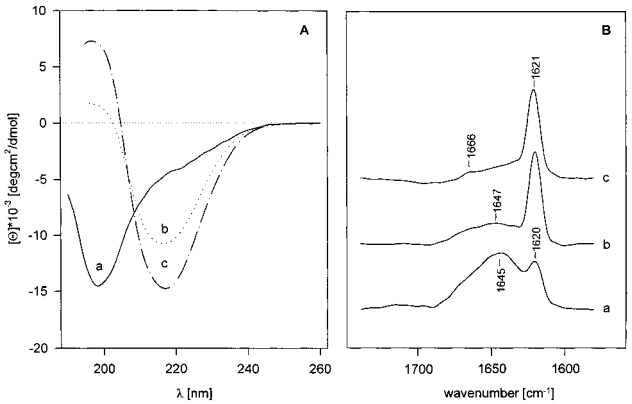

FIGURE 2: Influence of double D-amino acid substitution in the center of the $(VT)_n$-domain [VT6-DD (a), VT7-DD (b), VT8-DD (c)]. The conformation was studied by CD (A) in water at 5×10^{-5} M and FTIR (B) in D_2O buffer (30 mM sodium phosphate, pH 2.2) at a peptide concentration of 5×10^{-4} M. The FTIR spectra in the amide I region are shown after Fourier self-deconvolution.

analogue (Figure 2A, trace a) shows typical spectral features of unstructured peptides, indicating that D-amino acid substitution in the sequence with six VT-repeats leads to destruction of the β-sheet conformation. However, substitution in VT7, which is only one VT-repeat longer, is not sufficient to destroy the β-sheet conformation, as indicated by the negative feature at 218 nm (Figure 2A, trace b). The intensity of the minimum increases in the spectrum of VT8-DD (trace c), showing that the destabilizing influence of double D-amino acid substitution grows weaker according to the elongation and stabilization of the β-structured VT-region. However, the β-structures of the D-analogues differ from those formed by the L-analogues. The CD spectra of VT7-DD and VT8-DD show some special features which deviate from the spectra of VT7 and VT8 (compare traces e and f in Figure 1A with traces b and c in Figure 2A). The spectra of the D-peptides are slightly red-shifted, which is demonstrated by a shift of the minimum to 217 nm (from 214 nm) and of the crossover to 203−205 nm (from 200 nm). The intensities of the negative bands around 215 nm decrease in the case of the D-analogues, indicating destabilization of the β-structure.

The results of the infrared studies (Figure 2B), which are consistent with the CD data, also reveal an impact of D-amino acid substitution on the peptide conformation. At a concentration of 5×10^{-4} M the spectrum of the VT6-DD peptide (Figure 2B, trace a) is dominated by a broad amide I band centered at 1645 cm^{-1}, characteristic of unordered structures, plus a relatively weak feature at 1620 cm^{-1}. The latter indicates amide C═O groups in a β-sheet conformation, suggesting a concentration-dependent transition from random coil to β-sheet for this analogue. An amide I band at 1621 cm^{-1} dominates the FTIR spectra of the VT7-DD and VT8-DD peptides (Figure 2B, traces b and c). The amide I band at 1647 cm^{-1}, typical of an unordered structure, is almost absent in the spectrum of the VT8-DD peptide, indicating that the β-structure is stabilized. However, the high-frequency band at ~1690 cm^{-1} thought to be associated with antiparallel β-strands (*34*) is absent from the spectra of VT7-DD and VT8-DD. Although this might be an indication of a parallel β-structure (*35*), determination of the arrangement of the β-strands in VT-DD peptides is not possible on the basis of the present CD and IR data.

Association Behavior of the β-Structured Model Peptides. Sedimentation velocity and dynamic light scattering experiments were employed to monitor the association behavior of $(VT)_n$-peptides and their D-analogues (Table 2). These methods provide sedimentation ($s_{20,w}$) and diffusion coefficients ($D_{20,w}$). Time-resolved kinetics were observed with all peptide preparations by dynamic light scattering. The terminal value of the diffusion coefficient after 4 h is quoted as the equilibrium diffusion coefficient. To assess the degree of association, the molecular mass of the various assemblies was calculated from the sedimentation data. Unstructured peptides, VT3 and VT4, were found to be monomeric. Their molecular masses are close to the expected values. With VT5, which shows a concentration-dependent β-sheet structure, association starts abruptly (considerable change in the values of *s* and *D*). The molecular mass of the aggregate is determined to be more than 550 kDa, which represents an assembly of nearly 200 monomer units. The transition from VT5 to peptides with more than six VT-repeats provides a further strong increase of association. The stabilization of β-sheet structure in these peptides produces high molecular mass assemblies of more than 2000 kDa. Because these aggregates undergo sedimentation very rapidly, with broad distribution of the sedimenting species, large uncertainties in diffusion and sedimentation coefficients are observed. Therefore, molecular masses were estimated as average values. Considering the increasing sedimentation coefficients, and the decrease in diffusion coefficients from VT5 to VT8, it can be concluded that the degree of association correlates with the stabilization of the β-sheet structure.

D-Amino acid substitution influences the association behavior of VT-peptides in a different manner. Short β-sheet

Table 2: Association Behavior of $(VT)_n$-Peptides

peptide		analytical ultracentrifugation			dynamic light scattering
	M_r (kDa)	$s_{20,w}$ (S)	$D_{20,w}$ (10^{-7} cm^2/s)	$M_{r\,sD}$ (kDa)	$D_{20,w}$ (10^{-7} cm^2/s)
VT3	2.208	0.462 ± 0.005	18.80 ± 0.09	2.204 ± 0.027	
VT4	2.408	0.491 ± 0.016	17.87 ± 0.14	2.504 ± 0.102	
VT5	2.608	17.16 ± 0.05	2.85 ± 0.05	556.3 ± 11.6	1.35 ± 0.06
VT6	2.808	42.3 ± 1	1.54 ± 0.04	2000[a]	0.85 ± 0.06
VT7	3.008	70[a]	1−2[a]	2500[a]	0.42 ± 0.03
VT8	3.209	120[a]	<1[a]	>3000[a]	0.31 ± 0.02
VT5-DD	2.608	0.455 ± 0.055	15.7 ± 0.58	2.678 ± 0.438	
VT6-DD	2.808	10.2 ± 2	4 ± 1	240 ± 95	
VT7-DD	3.008	100[a]	<1[a]	2000[a]	1.34 ± 0.02
VT8-DD	3.209	130[a]	<1[a]	>2000[a]	

[a] Estimated values.

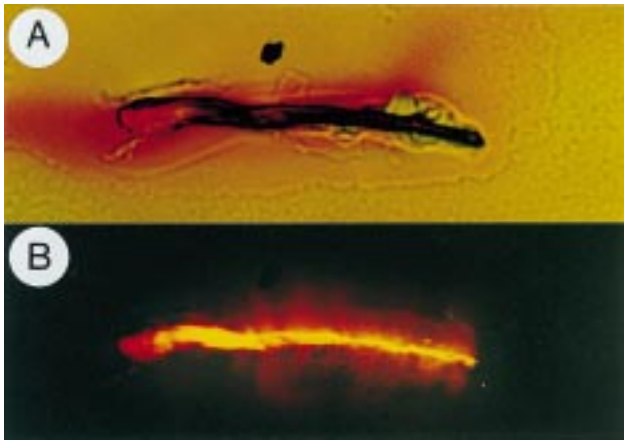

FIGURE 3: Birefringence of Congo Red-stained VT7 peptide aggregates: bright field (A) and polarized light (B). Magnification 400×.

structures are strongly disturbed in their association behavior, while the influence of longer sequences is weak. The missing β-sheet conformation in VT5-DD (*27*) agrees with the monomeric state of the peptide. The corresponding peptide (VT6-DD) having an additional VT-repeat was found to associate. However, the molecular mass of this assembly is about one magnitude smaller than that of its L-analogue. With elongation of the VT-domain ($n \geq 7$), association results again in high molecular mass assemblies (2000 kDa). However, despite the very large molecular mass of these assemblies, no precipitation was observed. The positive net charge at pH 4.4 leads to a certain stiffness of the aggregates which is reflected in the very low diffusion coefficients obtained by dynamic light scattering. When sodium chloride is added to the peptide solution, the charge-induced stiffness can be partially overcome, indicating an increase of the diffusion coefficient as determined by the analytical ultracentrifugation experiments. By means of sedimentation and diffusion coefficients and measurement of partial specific volume the frictional ratio can be calculated. Assuming ellipsoid revolution from the high frictional ratios of 1.7−2.0 for VT6, VT7, and VT6-DD, large axial ratios of 10:1 and 20:1 can be estimated.

Fibril Formation. To determine whether the peptides are organized into ordered quaternary structures, CR staining and electron microscopy were employed. These methods can provide indications of fibrillar structures and have also been used for investigations of amyloids. CR preferentially stains amyloids (*36*) but also binds to other fibrillar peptides (*37*). CR-stained amyloids show a green birefringence under polarized light, suggesting that the bound CR molecules are ordered with respect to each other. This effect is caused by the regular structure of the amyloids (*38*). The ability of high molecular mass VT-peptide assemblies to bind CR is shown in Figure 3. The stained peptide aggregates appear red (picture A) when observed by bright light optical microscopy and exhibit a yellow birefringence (picture B) under polarized light. Although the birefringence differs somewhat from the green birefringence of amyloids, it is a clear indication of their anisotropy and therefore indicates the presence of a regular quaternary structure.

Electron microscopy indicates a fibrillar structure for the high molecular mass VT-peptide assemblies (Figure 4). The

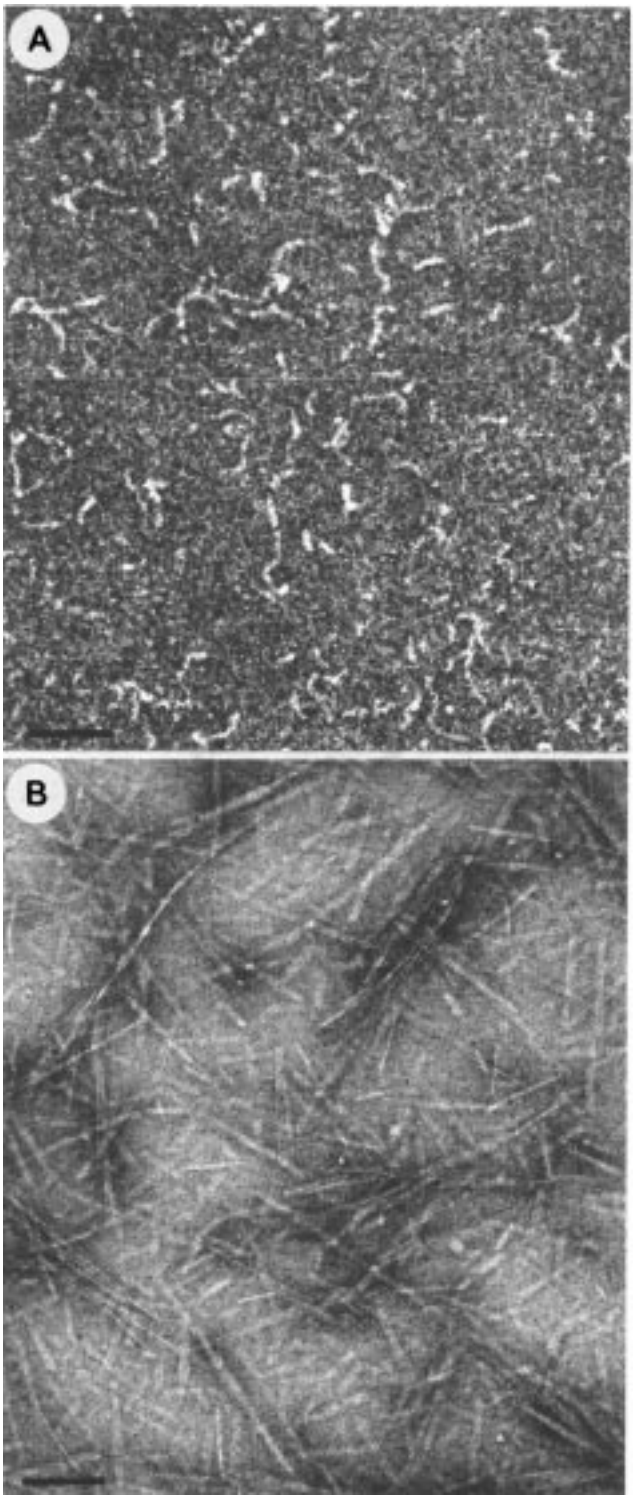

FIGURE 4: Electron microcraphs of negatively stained (2% uranyl acetate) fibrils from an aqueous solution (2×10^{-4} M) of peptide VT8 (A) and VT8-DD (B). Bar, 100 nm.

unbranched, wormlike fibrils are 7−9 nm in width and up to 100 nm in length (picture A). They are, in dimension, similar to fibrils of amyloidogenic peptides and proteins, which are 6−8 nm in width and 0.01−3 μm in length (*5*, *39*). Interestingly, D-amino acid substitution strongly influences the appearance of the fibrillar structures (picture B). Compared to fibrils of the nonsubstituted VT-peptides, the D-forms are of similiar width (5−7 nm) but much longer (up to 350 nm). The fibers are straight or only shlightly curved, suggesting a rigid molecular structure.

DISCUSSION

This report describes water-soluble de novo β-sheet peptides [DPKGDPKG-$(VT)_n$-GKGDPKPD-NH_2, $n = 3-8$] which self-assemble into fibrillar structures. The valine−threonine-based model peptides have enabled studies of the relationship between β-sheet stability and association. According to the hydrophobic−hydrophilic repeat pattern, matching a β-strand periodicity (*40*), and the high β-sheet propensities of valine and threonine (*41*−*44*), the peptides synthesized favor adoption of a β-sheet conformation. To overcome the handling problem regarding the formation of insoluble aggregates, which is a particular feature of sequences with β-periodicity and amphiphilic β-strands (*17*, *23*, *45*, *46*), the central $(Val\text{-}Thr)_n$ structure domain ($n = 3-8$) was flanked by two hydrophilic, unstructured octapeptide sequences which promote water solubility.

Conformational analyses (FTIR, CD) indicate differing potentials of the various peptides to adopt the β-sheet conformation. The critical chain length for a stable β-sheet formation in aqueous solution was found to be six VT-repeats (12 residues) which represent three VT-repeats (six residues) more than previously reported for amphiphilic oligopeptides containing valine and threonine (*43*). The observed increase in critical chain length can be attributed to the improved solubility, which is promoted by the N- and C-terminal octapeptide sequences. The stability of the β-sheet structure increases with elongation of the $(VT)_n$-domain to seven and eight repeats. Five VT-repeats represent a transition sequence from random coil to β-sheet structure. Sequences comprising less than five VT-repeats are unstructured. Once formed, the β-structure is highly stable. Attempts to disturb the conformation by temperature and the denaturant guanidine hydrochloride failed.

The association behavior was found to correlate strongly with peptide conformation. Unstructured peptides (three and four VT-repeats) are monomeric. On transition from a random coil to a β-sheet structure, association is initiated. Despite the weak β-sheet conformation determined for five VT-repeats, the molecular mass of the peptide assembly is very high (≈550 kDa). With stabilization of the β-sheet structure (from six to eight VT-repeats), association increases abruptly to high molecular mass species of more than 2000 kDa. Considering the small molecular mass of 2.6−3.2 kDa for the individual peptide chains, the size of the complex is immense. However, despite strong association, the β-sheet complexes are still water-soluble, and no precipitation occurs. This can be explained by the presence of unstructured octapeptides bearing a positive net charge which flank the aggregates.

The introduction of two adjacent D-amino acids was previously found to destroy α-helices (*32*, *33*) and weak β-sheet structures (*27*). In the present paper it has been shown that the influence of D-amino acid substitution is dependent on the stability of the β-sheet conformation. The destruction of the weak β-sheet structure with five VT-repeats (*27*) leads to monomeric species. Compared to the L-peptides, the beginning of β-sheet formation and association is shifted to the system having one VT-pair more (six VT-repeats). While this sequence adopts a very weak β-sheet conformation, the β-structure and association behavior of the longer domains with seven and eight repeats are only slightly destabilized. This is indicated especially by the high molecular masses of nearly 2000 kDa measured for these assemblies. Consequently, destabilization by D-amino acids has a greater effect on shorter sequences than on longer, more stable β-sheet domains.

Examination of the morphology of aggregation indicated that the high molecular mass species are organized into fibrillar structures, which show some similarities to those of amyloids, especially in terms of dimension and tinctorial properties (*2*, *4*, *5*, *39*). This fibrillar aggregation of de novo designed peptides suggests that the potential for amyloid formation is not restricted to peptides/proteins which are associated with amyloidoses and prion diseases but may be a common feature of a wide range of proteins. Interestingly, D-amino acid substitutions influence the morphology of β-sheet fibrils. In contrast to the wormlike fibrils of the nonsubstituted VT-peptides, these fibrils are straight and much longer. However, these differing characteristics cannot be explained on the basis of our conformational and association studies.

Because of the simplicity of these well-defined β-sheet model peptides, together with their excellent water solubility and similarity to amyloids, continued work in this field is planned. These studies will include an investigation of the influence of amino acid substitutions on the stability of intermolecular β-sheets as well as studies on the inhibition of fibrillar β-sheet complex formation.

ACKNOWLEDGMENT

We thank Christoph Böttcher for assisting cryoelectron microscopy experiments, Gerd Krause for computer modeling, Burkard Wiesner for help with the performance of light microscopy experiments, Bärbel Bödner and Heike Nikolenko for techniqual assistance, and Louis A. Carpino for critical reading of the manuscript.

REFERENCES

1. Prusiner, S. B. (1991) *Science 252*, 1515−1522.
2. Sipe, J. D. (1994) *Crit. Rev. Clin. Lab. Sci. 31*, 325−354.
3. Scherzinger, E., Lurz, R., Turmaine, M., Mangiarini, L., Hollenbach, B., Hasenbank, R., Bates, G. P., Davies, S. W., Lehrach, H., and Wanker, E. E. (1997) *Cell 90*, 549−558.
4. Glenner, G. G. (1980) *N. Engl. J. Med. 302*, 1283−1292.
5. Kelly, J. W. (1996) *Curr. Opin. Struct. Biol. 6*, 11−17.
6. Booth, D. R., Sunde, M., Bellotti, V., Robinson, C. V., Hutchinson, W. L., Fraser, P. E., Hawkins, P. N., Dobson, C. M., Radford, S. E., Blake, C. C., and Pepys, M. B. (1997) *Nature 385*, 787−793.
7. Soto, C., Castano, E. M., Kumar, R. A., Beavis, R. C., and Frangione, B. (1995) *Neurosci. Lett. 200*, 105−108.
8. Hilbich, C., Kisters Woike, B., Reed, J., Masters, C. L., and Beyreuther, K. (1992) *J. Mol. Biol. 228*, 460−473.
9. Fraser, P. E., McLachlan, D. R., Surewicz, W. K., Mizzen, C. A., Snow, A. D., Nguyen, J. T., and Kirschner, D. A. (1994) *J. Mol. Biol. 244*, 64−73.
10. Wood, S. J., Wetzel, R., Martin, J. D., and Hurle, M. R. (1995) *Biochemistry 34*, 724−730.
11. Sato, K., Wakamiya, A., Maeda, T., Noguchi, K., Takashima, A., and Imahori, K. (1995) *J. Biochem. 118*, 1108−1111.
12. Soto, C., Castano, E. M., Frangione, B., and Inestrosa, N. C. (1995) *J. Biol. Chem. 270*, 3063−3067.
13. Esler, W. P., Stimson, E. R., Ghilardi, J. R., Lu, Y.-A., Felix, A. M., Vinters, H. V., Mantyh, P. W., Lee, J. P., and Maggio, J. E. (1996) *Biochemistry 35*, 13914−13921.

14. Seilheimer, B., Bohrmann, B., Bondolfi, L., Müller, F., Stüber, D., and Löbeli, H. (1997) *J. Struct. Biol. 119*, 59−71.
15. Fabian, H., Choo, L.-P., Szendrei, G. I., Jackson, M., Halliday, W. C., Otvos, L., and Mantsch, H. H. (1993) *Appl. Spectrosc. 47*, 1513−1518.
16. Davis, J., and Van Nostrand, W. E. (1996) *Proc. Natl. Acad. Sci. U.S.A. 93*, 2996−3000.
17. Zhang, S., Holmes, T., Lockshin, C., and Rich, A. (1993) *Proc. Natl. Acad. Sci. U.S.A. 90*, 3334−3338.
18. Perutz, M. F., Johnson, T., Suzuki, M., and Finch, J. T. (1994) *Proc. Natl. Acad. Sci. U.S.A. 91*, 5355−5358.
19. Weaver, L., Stagsted, J., Behnke, O., Matthews, B. W., and Olsson, L. (1996) *J. Struct. Biol. 117*, 165−172.
20. Choo, D. W., Schneider, J. P., Graciani, N. R., and Kelly, J. W. (1996) *Macromolecules 29*, 355−366.
21. Symmons, M. F., Buchanan, S. G., Clarke, D. T., Jones, G., and Gay, N. J. (1997) *FEBS Lett. 412*, 397−403.
22. Blondelle, S. E., Forood, B., Houghten, R. A., and Perez Paya, E. (1997) *Biochemistry 36*, 8393−8400.
23. Lazo, N. D., and Downing, D. T. (1997) *Biochem. Biophys. Res. Commun. 235*, 675−679.
24. Aggelli, A., Bell, M., Boden, N., Keen, J. N., Knowles, P. F., McLeish, T. C., Pitkeathly, M., and Radford, S. E. (1997) *Nature 386*, 259−262.
25. Lim, A., Saderholm, M. J., Makhov, A. M., Kroll, M., Yan, Y. B, Perera, L., Griffith, J. D., and Erikson, B. W. (1998) *Protein Sci. 7*, 1545−1554.
26. Guijarro, J. I., Sunde, M., Jones, J. A., Campbell, I. D., and Doson, C. M. (1998) *Proc. Natl. Acad. Sci. U.S.A. 95*, 4224−4228.
27. Krause, E., Beyermann, M., Fabian, H., Dathe, M., Rothemund, S., and Bienert, M. (1996) *Int. J. Pept. Protein Res. 48*, 559−568.
28. Fabian, H., Schultz, C., Naumann, D., Landt, O., Hahn, U., and Saenger, W. (1993) *J. Mol. Biol. 232*, 967−981.
29. Behlke, J., and Ristau, O. (1997) *Biophys. J. 72*, 428−434.
30. Cohn, E. J., and Edsall, J. T. (1943) in *Proteins, Amino Acids and Peptides*, Academic Press, New York.
31. Nesloney, C. L., and Kelly, J. W. (1996) *Bioorg. Med. Chem. 4*, 739−766.
32. Krause, E., Beyermann, M., Dathe, M., Rothemund, S., and Bienert, M. (1995) *Anal. Chem. 67*, 252−258.
33. Rothemund, S., Beyermann, M., Krause, E., Krause, G., Bienert, M., Hodges, R. S., Sykes, B. D., and Sonnichsen, F. D. (1995) *Biochemistry 34*, 12954−12962.
34. Bandekar, J., and Krimm, S. (1986) *Adv. Protein Chem. 38*, 181−364.
35. Yamada, N., Ariga, K., Matsubara, K., and Koyama, E. (1998) *J. Am. Chem. Soc. 120*, 12192−12199.
36. Puchtler, H., Sweat, F., and Levine, M. (1962) *J. Histochem. Cytochem. 10*, 355−364.
37. Klunk, W. E. (1989) *J. Histochem. Cytochem. 37*, 1273−1281.
38. Cooper, J. H. (1974) *Lab. Invest. 31*, 232−238.
39. Lansbury, P. T., Jr. (1992) *Biochemistry 31*, 6865−6870.
40. Xiong, H., Buckwalter, B. L., Shieh, H. M., and Hecht, M. H. (1995) *Proc. Natl. Acad. Sci. U.S.A. 92*, 6349−6353.
41. Chou, P. Y., and Fasman, G. D. (1974) *Biochemistry 13*, 211−222.
42. Chou, P. Y., and Fasman, G. D. (1978) *Adv. Enzymol. Relat. Areas Mol. Biol. 47*, 45−148.
43. Altmann, K.-H., Flörsheimer, A., and Mutter, M. (1986) *Int. J. Pept. Protein Res. 27*, 314−319.
44. Smith, C. K., Withka, J. M., and Regan, L. (1994) *Biochemistry 33*, 5510−5517.
45. Osterman, D. G., and Kaiser, E. T. (1985) *J. Cell. Biochem. 29*, 57−72.
46. Hecht, M. H. (1994) *Proc. Natl. Acad. Sci. U.S.A. 91*, 8729−8730.

BI990510+